Proc. Natl. Acad. Sci. USA
Vol. 92, pp. 10879–10883, November 1995
Immunology

Mutagenesis in the C-terminal region of human interleukin 5 reveals a central patch for receptor α chain recognition

THOMAS MORTON, JUN LI, RICHARD COOK, AND IRWIN CHAIKEN*

Department of Molecular Immunology, SmithKline Beecham, 709 Swedeland Road, King of Prussia, PA 19406

Communicated by David R. Davies, National Institutes of Health, Bethesda, MD, July 17, 1995

ABSTRACT **Cassette mutagenesis was used to identify side chains in human interleukin 5 (hIL-5) that mediate binding to hIL-5 receptor α chain (hIL-5Rα). A series of single alanine substitutions was introduced into a stretch of residues in the C-terminal region, including helix D, which previously had been implicated in receptor α chain recognition and which is aligned on the IL-5 surface so as to allow the topography of receptor binding residues to be examined. hIL-5 and single site mutants were expressed in COS cells, their interactions with hIL-5Rα were measured by a sandwich surface plasmon resonance biosensor method, and their biological activities were measured by an IL-5-dependent cell proliferation assay. A pattern of mutagenesis effects was observed, with greatest impact near the interface between the two four-helix bundles of IL-5, in particular at residues Glu-110 and Trp-111, and least at the distal ends of the D helices. This pattern suggests the possibility that residues near the interface of the two four-helix bundles in hIL-5 comprise a central patch or hot spot, which constitutes an energetically important α chain recognition site. This hypothesis suggests a structural explanation for the 1:1 stoichiometry observed for the complex of hIL-5 with hIL-5Rα.**

Interleukin 5 (IL-5) plays a central role in the control of eosinophilia and as such is a major contributor to the tissue damage seen in asthma and other eosinophil-related disorders (1–4). The high-resolution crystallographic structure of human IL-5 (hIL-5) has been determined (5, 6). It contains a core of two four-helix bundles in the IL-5 dimer, with each of the four-helix units similar to that in other cytokines (7–11). However, the arrangement of bundles in IL-5 is unusual in that helix D of one monomer combines with helices A, B, and C of the second monomer and vice versa.

The hIL-5 receptor is composed of two types of subunits, denoted α and β (hIL-5Rα and -β) (12). The α chain is IL-5 specific and when expressed in a soluble form can bind to IL-5 without the β chain (12–14). In contrast, the β chain is identical to the β chain of granulocyte/macrophage colony-stimulating factor and IL-3 receptors (12, 15) and appears to be needed for signal transduction. Since the affinity of hIL-5 for the α chain is within an order of magnitude of that of the αβ heterocomplex (12, 16, 17), most of the binding energy for receptor binding appears due to the α chain.

A growing body of published evidence suggests that both helices A (residues 7–26) and D (residues 93–110) in IL-5 contribute important components to receptor binding sites for the α and β chains (18–21), but the structural mechanism by which the A and D helices participate in receptor interaction is not understood. Since IL-5 as a homodimer contains two A–D helix pairs (5), and each monomer is analogous to monomeric cytokines that can bind at least one receptor molecule [see, for example, de Vos *et al.* (22)], it might be expected that IL-5 could bind to two molecules of receptor α chain. However, an unexpected 1:1 stoichiometry for IL-5/IL-5Rα has been observed (6, 14).

The mechanism of IL-5 recognition of receptor α chain and the structural origin of 1:1 stoichiometry have formed a major focus for our mechanistic studies of hIL-5R recognition. In this study, we chose to investigate the effects of mutagenesis of residues in the C-terminal region of hIL-5 that includes helix D. This was based on a previous report (19) that used data from hybrid molecules of mouse–human IL-5 to suggest that the C-terminal region interacts directly with IL-5Rα and confers the species specificity of IL-5. We made sequence changes over a stretch of surface that extends from the distal ends of the two four-helix bundles of the IL-5 dimer inward to the interface between the bundles. This mutagenesis series allowed us to investigate both the importance of specific residues in the C-terminal region and the overall topography of the receptor recognition site on IL-5. The results show that the greatest impact of mutagenesis on receptor binding occurs for residues close together at the bundle interface, in particular Glu-110 and Trp-111. This observation suggests that a central recognition patch or hot spot exists on the AD side of hIL-5 that is important for receptor α chain interaction. The presence of a central patch may explain the unusual 1:1 stoichiometry observed for the hIL-5–α-subunit interaction.

MATERIALS AND METHODS

COS Expression of hIL-5. The gene for hIL-5 was placed behind a human tissue plasminogen activator secretion signal sequence in a *Drosophila* expression vector (6). The IL-5 gene with the signal sequence was cut from this vector by using *Eco*RI/*Bam*HI and ligated with the mammalian expression vector pCDN (SmithKline Beecham culture collection) behind a CMV promoter (pCDNIL5). This construction contains the full sequence of hIL-5 except that the N-terminal sequence was NH_2-GARSEIPTSALVKET (6). The GARS sequence was from the tissue plasminogen activator leader sequence used in expression. COS-1 cells were transfected with this construct using DEAE-dextran (23) and grown in serum-free medium. The level of expression was measured by using a Western blot probed with anti-hIL-5 antibody raised by immunization of rabbits with denatured fusion protein (expressed in *Escherichia coli* and gel purified) carrying hIL-5 sequence.

Mutagenesis. Site-directed mutagenesis was carried out by inserting a mutagenic cassette (24) into the two restriction sites of the template (pCDNIL5) closely flanking the IL-5 gene mutation target. Expression of the mutants was similar to that for wild type (wt) IL-5. Presence of the desired mutation was verified by DNA sequencing. Mutation sites are shown in Fig. 1.

Physical Characterization of Mutants. SDS/PAGE methods were used to verify that the mutants were folded into stable

The publication costs of this article were defrayed in part by page charge payment. This article must therefore be hereby marked "*advertisement*" in accordance with 18 U.S.C. §1734 solely to indicate this fact.

Abbreviations: hIL-5, human interleukin 5; (s)hIL-5Rα, (soluble) human IL-5 receptor α chain; wt, wild type.

*To whom reprint requests should be sent at the present address: Rheumatology Division, 913 Stellar Chance Laboratories, University of Pennsylvania School of Medicine, 422 Curie Boulevard, Philadelphia, PA 19104.

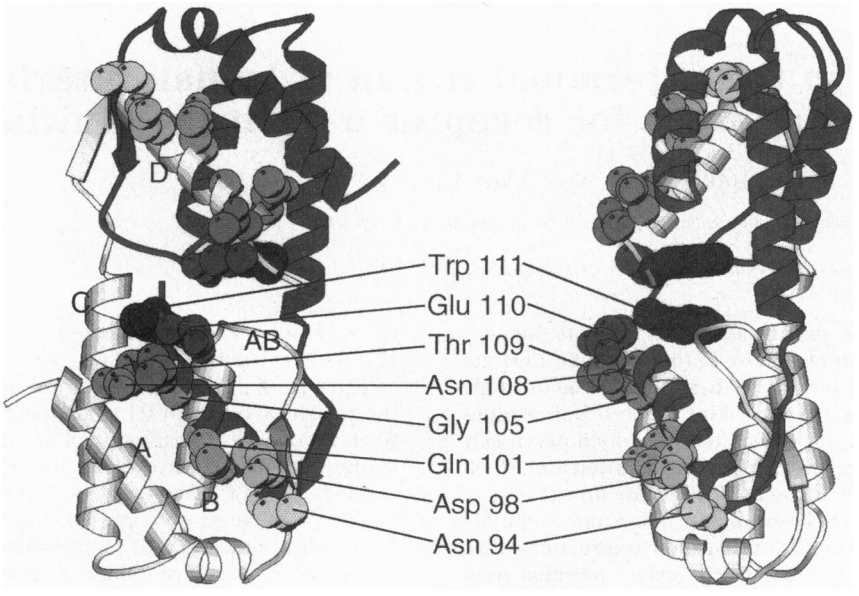

FIG. 1. Structural diagram of hIL-5 showing location of residues in D helices that were targets of mutagenesis. Figure identifies helices as A–D in each bundle and, as AB, the loop between helices A and B. Right and left sides are rotated 90° with respect to each other to show more clearly the residue locations on the AD face.

dimers at the COS expression supernatant stage. Dimer formation was determined by detecting a band of ≈33 kDa under nonreducing conditions (vs. ≈16 kDa under reducing conditions) in Western blots of SDS/polyacrylamide gels. The overall stability of the various mutant forms of IL-5 was tested by measuring the effect of urea on reduction of disulfide bonds and consequent dissociation of dimer. Urea was added to expression supernatants at concentrations up to 5 M in the presence of 0.3 mM dithiothreitol. After 1 hr at room temperature, the reaction mixture was quenched with 0.1 M iodoacetamide, and the mixture was run on nonreducing SDS/15% polyacrylamide gel. A Western blot of the gel was probed with anti-hIL-5 antiserum (6). The presence of monomer was taken to indicate that the urea had unfolded the IL-5, allowing the disulfides to be reduced by the dithiothreitol.

Receptor Binding Analysis of Mutants in Crude Expression Supernatants. Kinetics and equilibrium constants for the interaction between the mutant forms of hIL-5 and receptor were measured with a BIAcore optical biosensor. The nonneutralizing monoclonal antibody 24G9 (25) was first immobilized onto the biosensor chip. The expressed hIL-5 from COS supernatants was anchored noncovalently to the antibody. The binding of various concentrations of soluble hIL-5Rα (shIL-5Rα) [*Drosophila* expressed (6)] to the antibody-anchored hIL-5 was then measured. This arrangement avoids measuring the interaction in the presence of the large refractive index change caused by the COS medium and does not require determining the concentration of the anchored IL-5. Binding of antibody 24G9 to both wt hIL-5 and to the mutants tested in this study was similarly tight, with a very slow off rate; hence, the antibody effectively anchored the IL-5 without blocking its binding to receptor α chain. However, since the anchoring was noncovalent, there was expected to be a slow dissociation of IL-5 from the sensor surface. Given the above off-rate estimate, at least 90% of hIL-5 remained bound to 24G9 during the whole assay period. The slow dissociation of hIL-5 led to a slight overestimate of k_{off} (≤6% less) and underestimate of k_{on} (<1%). This had essentially no effect on the relative order of binding affinities observed for the various mutants.

For the sensor assays, 2 μl containing 2.4 μg of antibody 24G9 was diluted in 90 μl of 10 mM acetate (pH 4.5) and then injected on a sensor surface that had been preactivated with *N*-ethyl-*N'*-(3-diethylaminopropyl)carbodiimide/*N*-hydroxysuccinimide. After deactivation, 30 μl of IL-5 in cell-free COS supernatant was injected, followed by 30 μl of shIL-5Rα (0–30 nM for the higher-affinity mutants of IL-5 and 0–1.2 μM for the lower-affinity forms of IL-5). After each measurement, the surface was regenerated with 100 mM phosphoric acid. Regeneration removed both IL-5 and receptor. Hence, IL-5 was rebound to measure the binding at each different receptor concentration. The BIAcore data obtained were zeroed by subtracting the sensorgram recorded at 0 M receptor and then analyzed by least-squares fit of the data to a bimolecular (A + B to AB) model as described by Karlsson *et al.* (26). K_d values were determined from k_{off}/k_{on} ratios. Since the bimolecular model is viewed as an approximation for the biosensor interaction of hIL-5 with shIL-5Rα (6, 27), the rates and K_d values reported are taken as apparent. The variation of the apparent K_d values determined by this method is within 20% as judged from repeat assays using wt IL-5.

B13 Cell Proliferation Assay for Signal Transducing Activity of hIL-5 Mutants. hIL-5 can bind to murine IL-5R and hence was assayed for bioactivity by cell proliferation using the murine IL-5/IL-3 dependent B-cell line LyH7.B13 (6). The concentration of hIL-5 or hIL-5 mutant in COS supernatants used for these assays was estimated by Western blot analysis. Results are presented as percentage of the response ± SE obtained with wt hIL-5.

RESULTS

Expression, Folding, and Stability of Helix D Mutants. All of the mutants made in this study were expressed and secreted in roughly equal amounts (≈10 nM) in COS cells as judged by Western blot analysis of SDS/polyacrylamide gels. In all cases, the band detected under nonreducing conditions ran at ≈33 kDa, while that detected under reducing conditions was at ≈16 kDa. Hence, similar to wt hIL-5, all of the helix D mutants made were capable of folding into disulfide-linked dimers. The degree of susceptibility to urea-induced unfolding for the wt hIL-5 and mutants showed that all retained similar levels of overall stability. As shown in Fig. 2, tracking the extent of conversion of dimer to monomer as a function of urea concentration allowed an estimate of the extent of stability as measured by the amount of urea needed to convert half of the expressed hIL-5 to monomer. The wt IL-5 was half unfolded

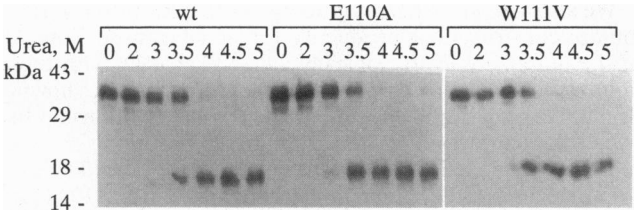

FIG. 2. Comparison of urea stability between wt and mutant hIL-5 (E110A, W111V). Concentrated COS cell supernatants (4 μl; 5-fold concentrated) were incubated with urea and 0.3 mM dithiothreitol, the reactions were stopped with iodoacetamide, and the mixtures were run on a nonreducing SDS/15% polyacrylamide gel followed by Western blot analysis.

in 3.5 M urea, as judged by the presence of approximately half of the Western-stained protein as monomer and half as dimer. This result is comparable to that seen for purified, *Drosophila*-expressed hIL-5 and for all of the mutants, with the possible exception of W111A. The latter appeared converted to slightly more than half monomer at 3.5 M urea, nonetheless indicative of folding to form a stable dimer.

Receptor Binding Activities of Helix D Mutants. Kinetics of receptor binding were measured by using a sandwich biosensor assay that allowed hIL-5 in crude COS supernatants to be characterized without the necessity for purification by measuring the binding of shIL-5Rα to antibody-anchored hIL-5 or hIL-5 mutant. Representative sensorgrams for wt and mutant hIL-5 are shown in Fig. 3*A*. For all cases, sensorgrams were obtained at a series of shIL-5Rα concentrations, and the association and dissociation phases were analyzed as described (28) to determine k_{on} and k_{off}, respectively. For the case of wt IL-5, the increase in response units as a function of time, dR/dt, was plotted as shown in Fig. 3*B*; from the slopes of these plots, k_s values were obtained that were replotted vs. receptor concentration (Fig. 3*B Inset*) to yield k_{on}. The k_{off} value was determined from the $\ln(R1/Rn)$ plot shown in Fig. 3*C*. The on and off rates calculated are given in Table 1, as is the equilibrium dissociation constant K_d calculated from the off/on rate ratio.

As noted previously (28), linearization of kinetics data shown in Fig. 3 *B* and *C* reveals significant nonlinearity, in particular at the higher concentrations of receptor. Such nonlinearity is often seen in optical biosensor analyses of macromolecular interactions (28–30). To fit the association data in Fig. 3*B* in order to obtain k_s and hence k_{on} values, we used the linear portions of the dR/dt plots at higher R values (6, 28). For dissociation data in Fig. 3*C*, we used the data in the early phase to determine k_{off}. Despite the analytical uncertainty due to nonlinearity, the biosensor data obtained in this study allowed a comparison to be made between binding properties for all of the mutants, and this was not undermined by either nonlinear kinetics or for that matter the slow dissociation of IL-5 from the 24G9 anchor. The K_d determined for COS-expressed wt hIL-5 analyzed in crude supernatants was 3–6 nM, a value similar to that measured for purified hIL-5 by biosensor analysis and titration calorimetry (6, 28).

Hence, biosensor analysis was applied to the crude supernatants containing hIL-5 mutants to measure their receptor binding activities. Sensorgrams for a representative set of mutants are shown in Fig. 3*A*. Most of the mutants had quantitative receptor binding properties similar to those of wt hIL-5, indicating that Ala substitutions at the residues involved did not remove any structural elements critical for receptor binding. However, for two residues—namely, Glu-110 and Trp-111—Ala substitutions caused substantive decreases in receptor affinity. This can be seen visually in Fig. 3*A* as well as in the quantitative data in Table 1.

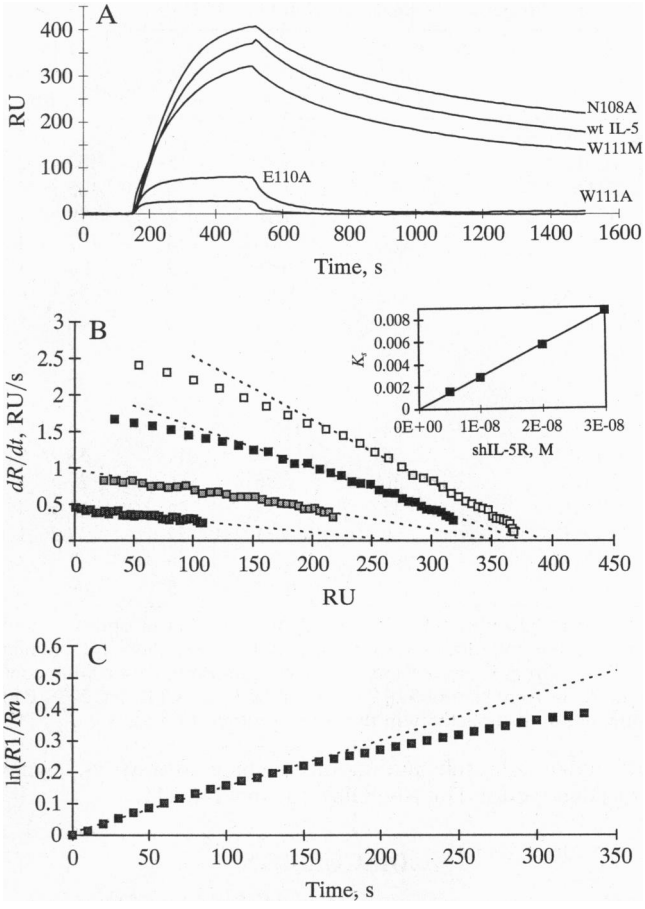

FIG. 3. Biosensor analysis of hIL-5–shIL-5Rα interaction. (*A*) Overlays of sensorgrams showing binding of various concentrations of shIL-5Rα to wt and various mutants of hIL-5. For wt IL-5, mutant N108A, and mutant W111M, 30 nM shIL-5Rα was used in the assay. For mutant E110A and W111A, 50 nM shIL-5Rα was used in order to see a detectable response. Increase in response shows the binding of shIL-5Rα. Decay represents dissociation of bound shIL-5Rα. (*B*) Calculation of on-rate constant for interaction of wt IL-5 with shIL-5Rα. Association phases of sensorgrams obtained at a series of shIL-5Rα concentrations were replotted as the slope of the curve at a given time vs. relative response (RU) at that time. From the straight line fit to the linear part of the data, the slopes give values for k_s at each concentration. (*Inset*) Plot of k_s vs. concentration. Slope of the line to these points gives the association rate constant. (*C*) Determination of dissociation rate constant for wt hIL-5. Dissociation phase of the sensorgram at 30 nM shIL-5Rα in *A* was replotted as ln(response at time 0 of dissociation/response at time *n*) vs. time. Straight line shows line fit to the early part of the data. Slope of the line gives dissociation constant.

In the case of Trp-111, several side chain types were examined for their ability to substitute for the indole of Trp-111. As shown in Table 1, several residues allowed a greater affinity of receptor binding than did Ala, with Met substitution yielding an affinity very close to that of wild type. There is a rough correlation between hydrophobic and space filling character of side chain at position 111 and the receptor affinity of the resultant mutant.

Signal Transduction. The ability of hIL-5 mutants to induce signal was measured by B-cell proliferation. Most of the mutants showed activities close to those of wt hIL-5 (Table 1). The three mutants with >50% reduction in activity—at Thr-109, Glu-110, and Trp-111—were also those with the greatest decrease in α chain interaction affinity. Hence, the decrease in activity observed with these mutants is likely due to the effect of the mutation on subsequent α chain interaction. Interestingly, though, there are quantitative differences in the relative

Table 1. Properties of single site mutants of hIL-5

	$k_{on} \times 10^{-3}$, $M^{-1}\cdot s^{-1}$	$k_{off} \times 10^{3}$, s^{-1}	K_d, nM	B13 stimulation, % wt hIL-5
Ala scan				
wt hIL-5	286	1.47	5	100 ± 2
N94A	236	1.05	4	105 ± 10
D98A	444	1.16	3	99 ± 1
Q101A	217	1.33	6	102 ± 4
G105A	309	0.56	2	84 ± 1
N108A	362	0.96	3	75 ± 6
T109A	170	2.11	12	46 ± 8
E110A	56	8.42	150	8 ± 2
W111A	86	13.6	158	44 ± 15
Trp-111 mutants				
W111A	86	13.6	158	44 ± 15
W111V	36	7.75	215	38 ± 9
W111Y	36	5.96	166	29 ± 1
W111L	45	2.89	64	60 ± 4
W111F	39	2.81	72	37 ± 1
W111M	201	1.25	6	137 ± 3
wt hIL-5	286	1.47	5	100 ± 2

Data are reported for two series of mutants, Ala substitutions and Trp-111 mutants. Rate constants k_{on} and k_{off} are those for binding shIL-5Rα from biosensor analysis, and equilibrium dissociation constant K_d is from the ratio k_{off}/k_{on}. SD of the K_d for wt IL-5 is 20%. B13 stimulation is the activity in the B-cell proliferation assay.

effects of Ala substitution on α chain affinity vs. signal transduction for Thr-109, Glu-110, and Trp-111.

DISCUSSION

Mutant Characterization Through Transient COS Expression. In this work, we used transient COS expression of hIL-5 mutants to examine the relative importance of a series of side chains in helix D for receptor binding and bioactivity of hIL-5 and used the results to evaluate the topography of the binding site for the IL-5-specific receptor subunit—namely, the α chain. Because of the number of mutants produced, we chose to determine their functional properties directly in COS supernatants rather than to purify each one separately. While this approach offered the benefit of being able to determine the role of a relatively large set of side chains, it required analytical methods that would not be compromised by the nonpurified state of the mutants.

The key methodology used to overcome such uncertainties was the biosensor sandwich assay, which was devised for the current study. This method allowed k_{on}, k_{off}, and consequent K_d to be measured by first trapping the IL-5 from COS supernatants selectively onto the sensor surface via immobilized nonneutralizing antibody 24G9. This entrapment is akin to an affinity purification directly on the sensor surface. 24G9 is a high-affinity, nonneutralizing monoclonal antibody to hIL-5 (25) and hence does not block subsequent binding of IL-5 to receptor.

Since binding to hIL-5Rα assumes that the ligand (wt or mutant hIL-5) is folded, it was necessary to confirm that the mutants, in particular those with low binding affinities, folded to a stable dimeric form. All of the mutants, including the low-activity E110A, W111A, and other Trp-111 mutants, formed dimers upon expression and were stable to urea concentrations at least to 3 M. This meant that the lower affinities observed with the latter mutants likely were not due to unfolding of the proteins during the sensor assay. Hence, loss of receptor binding activity could be interpreted directly as due to direct alteration by mutagenesis of the binding surface in hIL-5 for the receptor α chain.

We also assessed whether binding to hIL-5Rα by the various mutant constructs was productive for signal transduction. All of the mutants were biologically active (Table 1), with those mutants having a decreased receptor α chain affinity showing decreased signal transduction. However, the relationship between the reduction in receptor α chain interaction and reduction in bioactivity was not the same in all cases (Table 1). The reasons for this nonparallelism for T109A, E110A, and W111A cannot be defined at present but could reflect different mechanistic roles in such processes as receptor isomerization (6) or intracellular vs. extracellular receptor binding. However, we cannot exclude the possibility that the differences in relative binding affinity vs. bioactivity may have been due to differences in the receptor component (murine in the B-cell proliferation assay, human in the biosensor assay).

Selective Impact of Mutagenesis on Receptor Binding. The hIL-5 site-directed mutations investigated in this study were focused on residues in or near the solvent-exposed surface of the D helix and distributed along the helical axis from the distal ends of the helical bundles to the bundle–bundle interface. The residues chosen were substituted with Ala to minimize disruption of the D helix (31, 32). For residues close to the bundle–bundle interface, in particular Glu-110 and Trp-111 and to some extent Thr-109, changes in side chain character did impact both receptor α chain interaction and biological activity. Apparently, residues at the distal end of helix D play a less important role in receptor α chain recognition, while those near the bundle interface are more directly involved. Preliminary studies showed that mutants I112A and S115A also had affinities for shIL-5Rα similar to that of wt hIL-5. Hence, residues at the extreme C terminus of hIL-5, which are in a flexible peptide segment that extends away from the helix–bundle interface, also appear to be less directly involved in receptor α chain recognition.

The experimentally solved crystal structures of hIL-5 (5, 6) provide some clues as to the possible ways in which Glu-110 and Trp-111 could participate in receptor recognition. As shown in Fig. 1, the Glu-110 side chains are exposed to solvent, while those of Trp-111 are more buried. Glu-110 and perhaps Thr-109 may be contact residues for receptor and stabilize the receptor α chain complex directly. In contrast, the side chain of Trp-111 more likely functions as a packing residue to stabilize the local conformation of hIL-5 itself. Evidence for this hypothesis comes from the ability of hydrophobic residues such as Met to replace Trp with virtually unchanged receptor affinity. However, local disruption of the structure of the W111A form of hIL-5 is likely subtle, since the stability of this mutant in urea was only slightly reduced, at most, compared to wt hIL-5.

Topographical Mapping of Receptor Binding Sites: Central Patch and 1:1 Stoichiometry. The finding in this study that residues close to the bundle interface, in particular Glu-110 and Trp-111, are most important among helix D surface residues for receptor α chain interaction leads to the possibility that residues near the interface comprise a central patch that constitutes the α chain recognition site (Fig. 4). The central patch is envisioned as being localized on the side of the hIL-5 structure composed of exposed surfaces of the A and D helices, shown previously to be important for receptor ($\alpha\beta$ complex) interaction (18–20). The model of a central patch would explain the 1:1 stoichiometry observed for the complex of hIL-5 with hIL-5Rα in spite of the dimeric nature of hIL-5. Interestingly, Tavernier *et al.* (33) have recently reported that residues in the CD loop close to the four-helix bundle interface are part of the epitope for neutralizing antibody based on loss of antibody binding when residues in this loop are replaced. The results of neutralizing antibody epitope mapping suggest that the part of the CD loop closest to the bundle interface is at least close to, if not part of, the receptor binding site and suggests that the central patch may extend to include side chains in or close to the loop.

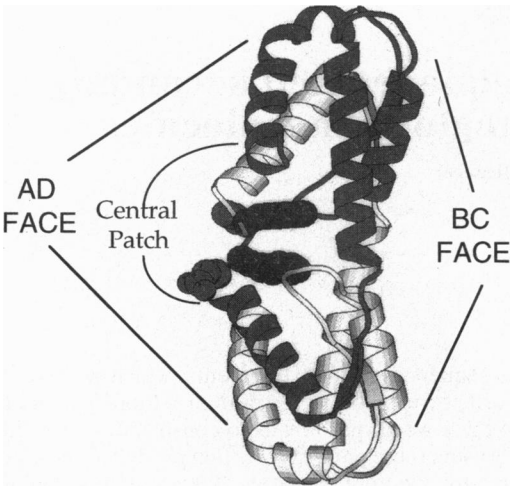

FIG. 4. Schematic view of hIL-5 showing various components of its surface. This scheme highlights regions hypothesized to be important in receptor recognition. (*i*) Central patch. This patch includes Glu-110, Trp-111, and residues around these including the AB loop. This patch appears to be important for α interaction. (*ii*) AD face. This side of the structure is dominated by the exposed surfaces of A and D helices. The A and D helices have been suggested in previous studies to be important for receptor binding. The involvement in receptor recognition of areas of this surface beyond the central patch remains to be determined. (*iii*) BC face. This side of the hIL-5 structure is dominated by the exposed surfaces of helices B and C. It is not known what role this surface plays in receptor recognition, but it is large, and residues in this face may be important for β chain interaction and consequently for signal transduction leading to biological activity.

The hypothesis of a central patch on hIL-5 for receptor α chain interaction is similar to the hot spot hypothesized on human growth hormone for its receptor (34). In the latter work, a central hydrophobic region dominated by two Trp residues accounted for more than three-fourths of the binding free energy. Interestingly, $\approx$30 growth hormone side chains overall make contact with receptor, and hence it may be concluded that side chains not in the hot spot also contribute to receptor recognition. A similar view may be suggested for IL-5—namely, that residues outside the central patch could still make receptor contact.

Overall, the data reported in this study provide a hypothesis for clustering of two Glu-110 and two Trp-111 residues in the hIL-5 dimer within a single binding site on the AD face for receptor α chain recognition. The results provide a framework in which to configure further mutagenesis studies—namely, to focus mutations to investigate (*i*) the composition and structural nature of the central patch, (*ii*) additional sites on the AD face that could participate in receptor α chain interaction, and (*iii*) the topography and role of residues that might be involved in β chain or other receptor interaction events. The hypothesis of a central patch, or hot spot, may help focus future efforts on the rational design of receptor antagonists for four-helix bundle cytokines of the IL-5 family (IL-3, IL-5, granulocyte/macrophage colony-stimulating factor), including muteins directed at residues outside the central patch and cytokine mimetics directed at structural elements within the central patch. The emerging view of receptor binding site topography also may provide insights into ways in which dimeric or multimeric receptor–cytokine complexes are formed, with applications not only for the IL-5 family of cytokines but also more generally for any four-helix bundle cytokine–receptor interaction.

We thank Ganesh Sathe, Joyce Mao, Stephanie Van Horne, and Rene Morris for their assistance with oligonucleotide synthesis and DNA sequencing.

1. Sanderson, C. J., Warren, D. J. & Strath, M. (1985) *J. Exp. Med.* **162,** 60–74.
2. Lopez, A. F., Sanderson, C. J., Gamble, J. R., Campbell, H. D., Young, I. G. & Vadas, M. A. (1988) *J. Exp. Med.* **167,** 219–224.
3. McKenzie, A. J. & Sanderson, C. J. (1992) in *Interleukins: Molecular Biology and Immunology*, ed. Kishimoto, T. (Karger, Basel), Vol. 51, pp. 135–152.
4. Bentley, A. M., Menz, G., Storz, C., Robinson, D. S., Bradley, B., Jeffery, P. K., Durham, S. R. & Kay, A. B. (1992) *Am. Rev. Respir. Dis.* **146,** 500–506.
5. Milburn, M. V., Hassell, A. M., Lambert, M. H., Jordan, S. R., Proudfoot, A. E. I., Graber, P. & Wells, T. N. C. (1993) *Nature (London)* **363,** 172–176.
6. Johanson, K., Appelbaum, E., Doyle, M., Hensley, P., Zhao, B., *et al.* (1995) *J. Biol. Chem.* **270,** 9459–9471.
7. Abdel-Meguid, S. S., Shieh, H.-S., Smith, W. W., Dayringer, H. E., Violand, B. N. & Bentle, L. A. (1987) *Proc. Natl. Acad. Sci. USA* **84,** 6434–6437.
8. Redfield, C., Smith, L. T., Boyd, J., Lawrence, G. M. P., Edwards, R. G., Smith, R. A. G. & Dobson, C. M. (1991) *Biochemistry* **30,** 11029–11035.
9. Diederichs, K., Boone, T. & Karplus, P. A. (1991) *Science* **254,** 1779–1782.
10. Powers, R., Garrett, D. S., March, C. J., Frieden, E. A., Gronenborn, A. M. & Clore, G. M. (1992) *Science* **256,** 1673.
11. Pandit, J., Bohm, A., Jancarik, J., Halenbeck, R., Koths, K. & Kim, S.-H. (1992) *Science* **258,** 1358–1362.
12. Tavernier, J., Devos, R., Cornelis, S., Tuypens, T., Van der Heyden, J., Fiers, W. & Plaetinck, G. (1991) *Cell* **66,** 1175–1184.
13. Murata, Y., Takaki, S., Migita, M., Kikuchi, Y., Tominaga, A. & Takatsu, K. (1992) *J. Exp. Med.* **175,** 341–351.
14. Devos, R., Guisez, Y., Cornelis, S., Verhee, A., Van der Heyden, J., Manneberg, M., Lahm, H. W., Fiers, W., Tavernier, J. & Plaetinck, G. (1993) *J. Biol. Chem.* **268,** 6581–6587.
15. Lopez, A. F., Elliott, M. J., Woodcock, J. & Vadas, M. A. (1992) *Immunol. Today* **13,** 495–500.
16. Tavernier, J., Tuypens, T., Plaetinck, G., Verhee, A., Fiers, W. & Devos, R. (1992) *Proc. Natl. Acad. Sci. USA* **89,** 7041–7045.
17. Takaki, S., Murata, Y., Kitamura, T., Miyajima, A., Tominaga, A. & Takatsu, K. (1993) *J. Exp. Med.* **177,** 1523–1529.
18. Kodama, S., Tsuruoka, N. & Tsujimoto, M. (1991) *Biochem. Biophys. Res. Commun.* **178,** 514–519.
19. McKenzie, A. N. J., Barry, S. C., Strath, M. & Sanderson, C. J. (1991) *EMBO J.* **10,** 1193–1199.
20. Shanafelt, A. B., Miyajima, A., Kitamura, T. & Kastelein, R. A. (1991) *EMBO J.* **10,** 4105–4112.
21. Goodall, G. J., Bagley, C. J., Vadas, M. A. & Lopez, A. F. (1993) *Growth Factors* **8,** 87–97.
22. de Vos, A. M., Ultsch, M. & Kossiakoff, A. A. (1992) *Science* **255,** 306–312.
23. Sussman, D. J. & Milman, G. (1984) *Mol. Cell. Biol.* **4,** 1641–1643.
24. Wells, J. A., Vasser, M. & Powers, D. B. (1985) *Gene* **34,** 315–323.
25. Ames, R. S., Tornetta, M. A., McMillan, L. J., Kaiser, K. F., Holmes, S. D., Appelbaum, E., Cusimano, D. M., Theisen, T. W., Gross, M. S., Jones, C. S., Silverman, C., Porter, T. G., Cook, R. M., Bennett, D. & Chaiken, I. M. (1995) *J. Immunol.* **154,** 6355–6364.
26. Karlsson, R., Michaelsson, A. & Mattsson, L. (1991) *J. Immunol. Methods* **145,** 229–240.
27. Morton, T., Myszka, D. G. & Chaiken, I. M. (1995) *Anal. Biochem.* **227,** 176–185.
28. Morton, T., Bennett, D. B., Appelbaum, E. R., Cusimano, D., Johanson, K. O., Matico, R. E., Young, P. R., Doyle, M. L. & Chaiken, I. M. (1994) *J. Mol. Recognit.* **7,** 47–55.
29. Bondeson, K., Frostell-Karlsson, A., Fagerstam, L. & Magnusson, G. (1993) *Anal. Biochem.* **214,** 245–251.
30. Zeder-Lutz, G., Altschuh, D., Geysen, H. M., Trifilieff, E., Sommer Meyer, G. & Van Regenmortel, H. V. (1993) *Mol. Immunol.* **30,** 145–155.
31. Komoriya, A. & Chaiken, I. M. (1982) *J. Biol. Chem.* **257,** 2599–2604.
32. Wells, J. A. (1991) *Methods Enzymol.* **202,** 390–411.
33. Tavernier, J., Guisez, Y., Devos, R., Plaetinck, G., Van der Heyden, J. & Oefner, C. (1994) in *Cytokines: Basic Principles and Practical Applications*, eds. Romagnani, S., Del Prete, G. & Abbas, A. K. (Ares-Serono Symposia, Boston), pp. 99–107.
34. Clackson, T. & Wells, J. A. (1995) *Science* **267,** 383–386.